

Regulation of KIF23 by miR-107 controls replicative tumor cell fitness in mouse and human hepatocellular carcinoma

Mirco Castoldi, Sanchari Roy, Carolin Angendoehr, Rossella Pellegrino, Mihael Vucur, Michael T. Singer, Veronika Buettner, Matthias A. Dille, Stephanie D. Wolf, Lara R. Heij, Ahmed Ghallab, Wiebke Albrecht, Jan G. Hengstler, Georg Flügen, Wolfram T. Knoefel, Johannes G. Bode, Lars Zender, Ulf P. Neumann, Mathias Heikenwälder, Thomas Longerich, Christoph Roderburg, Tom Luedde

Article - Version of Record



Suggested Citation:

Castoldi, M., Roy, S., Angendoehr, C., Pellegrino, R., Vucur, M., Singer, M. T., Büttner, V., Dille, M., Wolf, S. D., Heij, L. R., Ghallab, A., Albrecht, W., Hengstler, J. G., Flügen, G., Knoefel, W. T., Bode, J. G., Zender, L., Neumann, U. P., Heikenwälder, M., ... Lüdde, T. (2024). Regulation of KIF23 by miR-107 controls replicative tumor cell fitness in mouse and human hepatocellular carcinoma. *Journal of Hepatology*, 82(3), 499–511. <https://doi.org/10.1016/j.jhep.2024.08.025>

Wissen, wo das Wissen ist.

This version is available at:

URN: <https://nbn-resolving.org/urn:nbn:de:hbz:061-20250220-113056-1>

Terms of Use:

This work is licensed under the Creative Commons Attribution 4.0 International License.

For more information see: <https://creativecommons.org/licenses/by/4.0>

Regulation of KIF23 by miR-107 controls replicative tumor cell fitness in mouse and human hepatocellular carcinoma

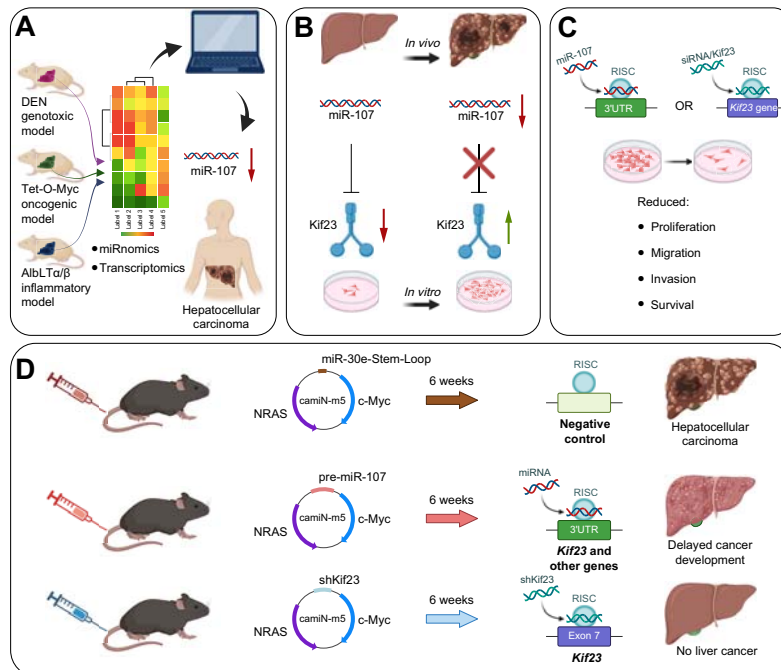
Authors

Mirco Castoldi, Sanchari Roy, Carolin Angendohr, ..., Mathias Heikenwalder, Thomas Longerich, Christoph Roderburg, Tom Luedde

Correspondence

mirco.castoldi@uni-duesseldorf.de (M. Castoldi), luedde@uni-duesseldorf.de (T. Luedde).

Graphical abstract



Highlights

- miR-107 is globally downregulated in mouse liver cancers of different etiologies and represents a potential biomarker in human HCC.
- KIF23 identified as a specific target mediating the biological effects of miR-107.
- The miR-107/KIF23 module promotes replicative fitness of liver cancer cells through an essential function in cytokinesis.
- Mice treated with a shRNA targeting Kif23 were completely protected from oncogene-induced liver cancer development.

Impact and implications

Our study revealed the central role of the miR-107/KIF23 axis in controlling tumor cell fitness and hepatocellular carcinoma progression. The results demonstrate that the overexpression of miR-107 or silencing of its target, KIF23, markedly suppresses the proliferation, survival, and motility of human and mouse hepatoma cells. In this work, we demonstrate that the disruption of miR-107/Kif23 signaling effectively protects mice from an aggressive form of oncogene-induced liver cancer *in vivo*, implying that targeting miR-107/KIF23 might be a novel therapeutic approach for hepatocellular carcinoma in humans.

Regulation of KIF23 by miR-107 controls replicative tumor cell fitness in mouse and human hepatocellular carcinoma

Mirco Castoldi^{1,2,*}, Sanchari Roy^{1,2}, Carolin Angendoehr^{1,2}, Rossella Pellegrino³, Mihael Vucur^{1,2}, Michael T. Singer^{1,2}, Veronika Buettner^{1,2}, Matthias A. Dille^{1,2}, Stephanie D. Wolf^{1,2}, Lara R. Heij^{4,5,6}, Ahmed Ghallab^{7,8}, Wiebke Albrecht⁷, Jan G. Hengstler⁷, Georg Flügen^{5,9}, Wolfram T. Knoefel⁹, Johannes G. Bode^{1,2}, Lars Zender¹⁰, Ulf P. Neumann^{4,5}, Mathias Heikenwälder¹¹, Thomas Longerich³, Christoph Roderburg^{1,2,§}, Tom Luedde^{1,2,*}

Journal of Hepatology 2025. vol. 82 | 499–511



See Editorial, pages 414–416

Background & Aims: In hepatocellular carcinoma (HCC), successful translation of experimental targets identified in mouse models to human patients has proven challenging. In this study, we used a comprehensive transcriptomic approach in mice to identify novel potential targets for therapeutic intervention in humans.

Methods: We analyzed combined genome-wide miRNA and mRNA expression data in three pathogenically distinct mouse models of liver cancer. Effects of target genes on hepatoma cell fitness were evaluated by proliferation, survival and motility assays. TCGA and GEO databases, in combination with tissue microarrays, were used to validate the mouse targets and their impact on human HCC prognosis. Finally, the functional effects of the identified targets on tumorigenesis and tumor therapy were tested in hydrodynamic tail vein injection-based preclinical HCC models *in vivo*.

Results: The expression of miR-107 was found to be significantly reduced in mouse models of liver tumors of various etiologies and in cohorts of humans with HCC. Overexpression of miR-107 or inhibition of its novel target kinesin family member 23 (Kif23) significantly reduced proliferation by interfering with cytokinesis, thereby controlling survival and motility of mouse and human hepatoma cells. In humans, KIF23 expression was found to be a prognostic marker in liver cancer, with high expression associated with poor prognosis. Hydrodynamic tail vein injection of vectors carrying either pre-miR-107 or anti-Kif23 shRNA inhibited the development of highly aggressive c-Myc-NRAS-induced liver cancers in mice.

Conclusions: Disruption of the miR-107/Kif23 axis inhibited hepatoma cell proliferation *in vitro* and prevented oncogene-induced liver cancer development *in vivo*, offering a novel potential avenue for the treatment of HCC in humans.

© 2024 The Authors. Published by Elsevier B.V. on behalf of European Association for the Study of the Liver. This is an open access article under the CC BY license (<http://creativecommons.org/licenses/by/4.0/>).

Introduction

Hepatocellular carcinoma (HCC) represents the most common type of primary liver cancer.¹ Despite recent advances in the systemic treatment of advanced HCC through immune checkpoint inhibition,^{2,3} long-term survival remains limited in most patients.⁴ In many non-oncological but also certain oncological diseases, it has been suggested that not a single treatment but the combined targeting of various vulnerable disease mechanisms could lead to a decisive breakthrough.⁵ In the case of HCC, for example, this could lie in the synchronous or staggered combination of immunotherapies with the targeting of other vulnerable disease mediators.⁶ The basis for such innovative concepts would be the identification of new targets with relevance in human patients. However, a large gap still exists between the amount of

experimental findings in HCC model systems and their successful translation into a clinical context.

MicroRNAs (miRNAs) are key epigenetic regulators of the transcriptome, whose dysregulation has been linked to the control of several oncogenic hallmarks.⁷ Although a large and growing body of literature indicates that dysregulation of miRNA expression plays an important role in hepatocarcinogenesis,⁸ the success of translating miRNA-centered animal studies into clinical trials in humans has been hampered by an inadequate ability to predict the human response to treatment. HCC in humans is characterized by wide inter- and intra-tumor heterogeneity.⁹ Since individual animal models can reflect only some molecular aspects of human HCC pathogenesis, it is currently unclear which animal model of liver cancer is best suited for studying molecular

* Corresponding authors. Address: Moorenstr. 5, 40225 Düsseldorf, Germany.

E-mail addresses: mirco.castoldi@uni-duesseldorf.de (M. Castoldi), luedde@uni-duesseldorf.de (T. Luedde).

§ Shared last authorship

<https://doi.org/10.1016/j.jhep.2024.08.025>



mechanisms of significant relevance to humans. miRNAs, while not directly functional mediators, regulate cellular physiology by fine-tuning gene expression within larger regulatory networks.¹⁰ Their analysis may therefore reveal potential therapeutic targets. To identify dysregulated miRNA networks relevant to human liver cancer development, systems biology approaches were used to analyze and correlate the miRnome and transcriptome in mouse models of liver cancer.¹¹ In the present study, we combined *in silico* prediction with comprehensive miRNA and mRNA transcriptomic analysis and identified miR-107 as globally down-regulated in HCC. We found that miR-107 controls the migration and invasion of liver cancer cells through the fine-tuning of kinesin family member 23 (KIF23), a spindle-associated motor protein critical for cytokinesis,¹² representing a promising biomarker and therapeutic target in human HCC.

Materials and methods

Data retrieval from the GEO repository and analysis

The miRNA and mRNA profiling data in animal models of liver cancer were retrieved from the GEO (Gene Expression Omnibus)¹³ under the super-series accession number GSE102418. This super-series is composed of the following sub-series: GSE102416, which contains the raw data from the analysis of miRNA expression, and GSE102417 that contains the CEL files from the Affymetrix microarray. CEL files were analyzed using the comprehensive transcriptome analysis software AltAnalyze version 2.1.3,¹⁴ with a fold-change cut-off of ≥ 2 and a $p \leq 0.05$. For the purpose of this analysis, arrays from mice treated with diethylnitrosamine (DEN), transgenic overexpression of lymphotoxin (AlbLT α/β) and Tet-O-Myc were grouped as normal, non-tumor liver (NTL) and tumor liver, regardless of pathogenesis. Enrichment analysis was performed with ShinyGO¹⁵ by uploading a list of significantly upregulated genes, which were predicted to be miR-107 targets by miRWalk¹⁶ target prediction database. The Disease.Jensen.DISEASES database, which is linked to the ShinyGO platform, was used to identify diseases associated with miR-107 predicted targets upregulated in the tumor tissues of the three mouse models of HCC, based on adjusted p values. Intersections between the microarray data and the miRWalk-generated list of miR-107 predicted targets were identified using the Venny Venn diagram (<https://bioinfogp.cnb.csic.es/tools/venny/>).

Human liver samples

Different cohorts of resected liver samples from patients with HCC were analyzed in this study. **Table S1A:** Unpaired cohort, consisting of unpaired tumor and healthy tissue from different donors ($n = 7$ per group; previously described in¹⁷). **Table S1B:** Paired cohort, consisting of paired tumor and distal healthy tissue from the same donors ($n = 9$). **Table S1C:** Tissue microarray (TMA) cohort, including tumor and surrounding liver tissue from the same donors ($n = 62$).

Liver TMA

The liver TMA containing non-tumorous and tumor liver tissues from patients with HCC (**Table S1C**) was constructed as previously described,¹⁸ using liver samples provided by the Institute of Pathology, RWTH Aachen. Immunohistochemistry was

performed on 3 μm sections. Antigen retrieval was carried out using citrate buffer solution pH 6 (Dako, Glostrup, Denmark). Detection was performed using the EnVision method (Dako) and counterstaining was done with hemalum solution. Staining was assessed using the immunoreactive score as previously described¹⁹: Primary antibody used to stain the TMAs: anti-KIF23 (1:100, Abcam Cambridge, MA, USA, ab174304). TMA scoring: 0, absent; 1–4, weak; 5–8, moderate; 9–12, strong expression.

Ethics approval

The relevant official authority for animal protection (Landesamt für Natur, Umwelt und Verbraucherschutz Nordrhein-Westfalen, Recklinghausen, Germany) approved this study (reference number 84-02.04.2011.A133). Animals received care according to the German animal welfare act. Animal experiments included in this study were carried out in compliance with the Act No 246/1992 Coll. The Ethics Committees of the Medical Faculties of Düsseldorf (vote number 2022-1848 and 2017-4664) and RWTH Aachen (vote number EK206/09) approved the use of human HCC tissue samples in accordance with the ethical guidelines of the Declaration of Helsinki. All patients included in the study provided written informed consent. The TMA was prepared with liver tissues provided by the Institute of Pathology, RWTH Aachen, and their use was approved by the local ethics committee in accordance with the Declaration of Helsinki (vote number EK122/16).

Analyses of TCGA data and Kaplan-Meier survival curves

Some of the results shown in this study are based upon data generated by The Cancer Genome Atlas (TCGA) Research Network: <https://www.cancer.gov/tcga> (accessed on 7th of April 2023). Kaplan-Meier survival curves of patients with liver hepatocellular carcinoma (LIHC) for the selected genes were generated using the Kaplan-Meier plotter.²⁰ A multivariate analysis using Cox proportional hazards regression was performed on the survival curves of miR-107 and KIF23 in patients with LIHC using cSurvival.²¹

Statistical analysis and imaging software

Statistical analyses were carried out using GraphPad Prism (version 9.4.1). To evaluate whether samples were normally distributed, the D'Agostino and Pearson normality tests were carried out. When the sample distribution passed the normality test, then parametric tests were carried out (*i.e.*, one-way analysis of variance/ANOVA for three or more samples and a two-tailed t test for two samples). In cases in which the samples did not pass the normality test, non-parametric tests were applied (*i.e.*, the Kruskal–Wallis test for three or more samples and the Mann-Whitney test for two samples). Paired samples were analyzed using the Wilcoxon signed-rank test. The data were considered significant at a p value ≤ 0.05 . Images were prepared using Affinity Designer (version 2.5.0). Data were analyzed using GraphPad Prism (GraphPad Software, Inc., La Jolla, CA, Version 9.4.1).

Additional methods

The supplementary materials and methods section provides information on additional methods used to prepare, culture, treat,

and analyze both primary cells and cell lines. This section also includes detailed methods used to perform transfection, RNA and protein isolation, cDNA synthesis, reverse-transcription quantitative PCR, and western blotting. Additional information is also available in the supplementary CTAT table.

Results

miR-107 is downregulated in mouse and human liver cancer

We analyzed genome-wide data on miRNA expression in liver cancers of mice from three prototypical models for liver cancer formation (DEN as a model of genotoxic hepatocarcinogenesis; AlbLT α/β as an inflammatory HCC model; and the oncogene-driven c-Myc model [Tet-O-Myc mice]).¹¹ This analysis revealed a common downregulation of miR-107 whose function

in hepatocarcinogenesis was not known (Fig. 1A). First, we measured and validated the downregulation of miR-107 expression in the livers of the three mouse models used in the genome-wide analysis (Fig. 1B,C). We also corroborated these results by measuring the expression of miR-107 in the tumor tissue of other well-established mouse genetic models of liver cancer (namely: Tak1^{LPC-KO},^{22,23} Mcl-1 ^{Δ hep},²⁴ Mdr2^{-/-25} and Traf2/Ripk1^{LPC-KO26} mice; Fig. 1D), and found that miR-107 was significantly downregulated in the tumors of all these respective animal models of HCC that we had analyzed.

We next assessed miR-107 levels in various mouse (Hepa 1-6, Hepa1c1c7) and human (Huh-7, HepG2) hepatoma cell lines and compared them to the expression in normal mouse and human livers, respectively. Consistent with the findings in murine liver cancer models, we observed a significant downregulation of miR-107 in both mouse Hepa1c1c7 and human Huh-7 hepatoma cell lines when compared to their respective

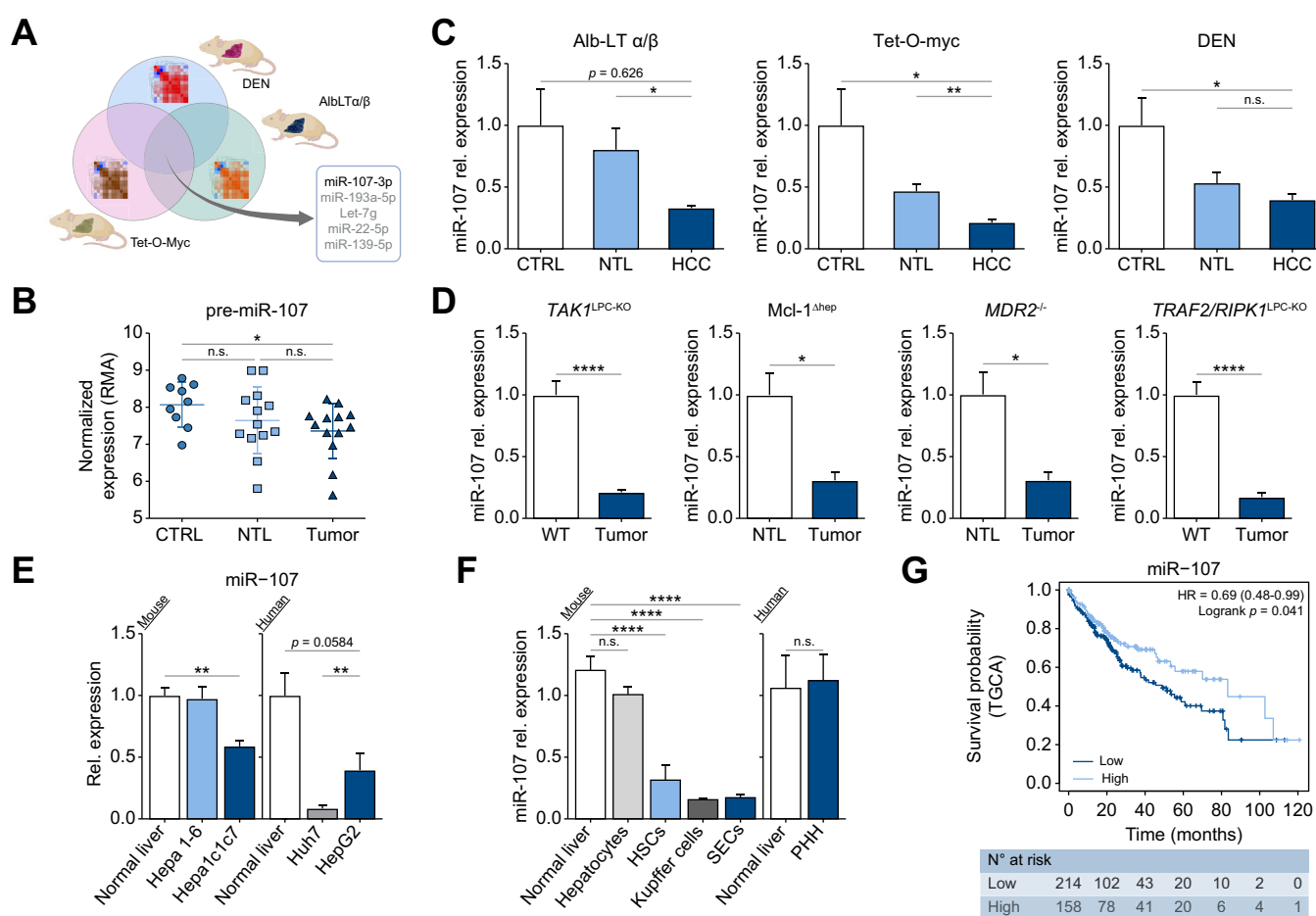


Fig. 1. miR-107 is globally downregulated in etiologically unrelated mouse model of liver cancer and in human. (A) Systems biology was employed to globally identify miRNAs that were downregulated in the tumor tissues of three etiologically distinct mouse models of liver cancer: DEN, AlbLT α/β , and Tet-O-Myc. (B) RMA-normalized microarray data for the expression of pre-miR-107 in the healthy (n = 9), NTL (n = 13) and tumor liver tissue (n = 13) from the mice included in this study. (C) RT-qPCR validation of miR-107 expression in the individual DEN (untreated, n = 6; NTL, n = 5; tumor, n = 5), AlbLT α/β (untreated, n = 4; NTL, n = 4; tumor, n = 4), and Tet-O-Myc (untreated, n = 4; NTL, n = 4; tumor, n = 4) models of liver cancer. (D) RT-qPCR analysis of miR-107 in four different genetic HCC mouse tumor models: Mcl-1 ^{Δ hep} (n = 5), TAK1-KO (n = 11), TRAF2-RIPK1-KO (n = 7), Mdr2-KO (n = 7) compared to either NTL or WT mice. (E) RT-qPCR of miR-107 expression in normal mouse (n = 5) and human (n = 3) livers and in mouse (Hepa1-6; n = 5, Hepa1c1c7; n = 5) and human hepatoma cells (Huh-7; n = 5, HepG2; n = 5, Hep3B; n = 5). (F) RT-qPCR of miR-107 expression in cells isolated from the livers of WT mice and from human primary hepatocytes. Mouse liver cells n = 4 per cell type. Human normal livers n = 7, PHHs n = 6. (G) Kaplan-Meier curves for the overall survival of patients with HCC plotted against time (months) based on miR-107 expression levels (TCGA-LIHC cohort datasets; n = 372). Results are represented as mean \pm SD, significant differences were evaluated by using one-way ANOVA with Newman-Keuls *post hoc* test or two-tailed, unpaired t test as appropriate. * $p \leq 0.05$; ** $p \leq 0.001$; **** $p \leq 0.0001$. DEN, diethylnitrosamine; HSCs, hepatic stellate cells; NTL, non-tumoral liver; PHHs, primary human hepatocytes; SECs, sinusoidal endothelial cells; WT, wild-type.

controls (Fig. 1E). To evaluate miR-107 expression levels in different liver cell types, we analyzed primary hepatocytes, hepatic stellate cells, sinusoidal endothelial cells, and Kupffer cells from mouse livers. Notably, miR-107 expression was significantly lower in hepatic stellate cells, Kupffer cells, and sinusoidal endothelial cells compared to primary mouse hepatocytes, suggesting that miR-107-mediated silencing of its transcriptional network may play a specifically crucial role in these respective cells (Fig. 1F, left panel). Notably, in accordance with the measurement in the mouse, no significant differences in miR-107 expression were observed in primary human hepatocytes compared to normal human liver (Fig. 1F, right panel). To further explore the possible correlation between liver cancer development and miR-107 expression in humans, we conducted an analysis using LIHC cohorts sourced from "The Cancer Genome Atlas" (TCGA) database. By employing Kaplan-Meier curves to assess patient survival, our study revealed a significant association between decreased expression of miR-107 and a significantly shorter survival in patients with HCC (Fig. 1G). These findings underscore the potential significance of miR-107 in the progression of HCC in humans.

miR-107 upregulation negatively impacts the replicative fitness of human and mouse hepatoma cells

To unveil the functional role of miR-107 in liver cancer, we assessed its impact on the oncogenic hallmarks of cancer cells, such as cellular proliferation, survival, and motility. In human Huh-7 hepatoma cells, we found that miR-107 overexpression significantly inhibited the cells' ability to proliferate and migrate, ultimately reducing their overall survival (Fig. 2A–G). Specifically, we found that increased levels of miR-107 impaired Huh-7 colony formation (Fig. 2A), proliferation (Fig. 2B,C), cell death (Fig. 2D), and motility (Fig. 2E–G). Overall, these results suggest that elevated levels of miR-107 significantly reduce the overall fitness of human hepatoma cells. These findings were confirmed in human HepG2 (Fig. S1A–C) and in murine Hepa1c1c7 (Fig. S2A–G) hepatoma cells. Overexpression of miR-107 in these cell lines resulted in comparable outcomes to those observed in Huh-7 hepatoma cells, including similar effects on cellular proliferation, survival, and motility. These data support the conclusion that, in addition to inhibiting cell proliferation and inducing cell death, miR-107 overexpression inhibits the migration and invasion capabilities of hepatoma cells.

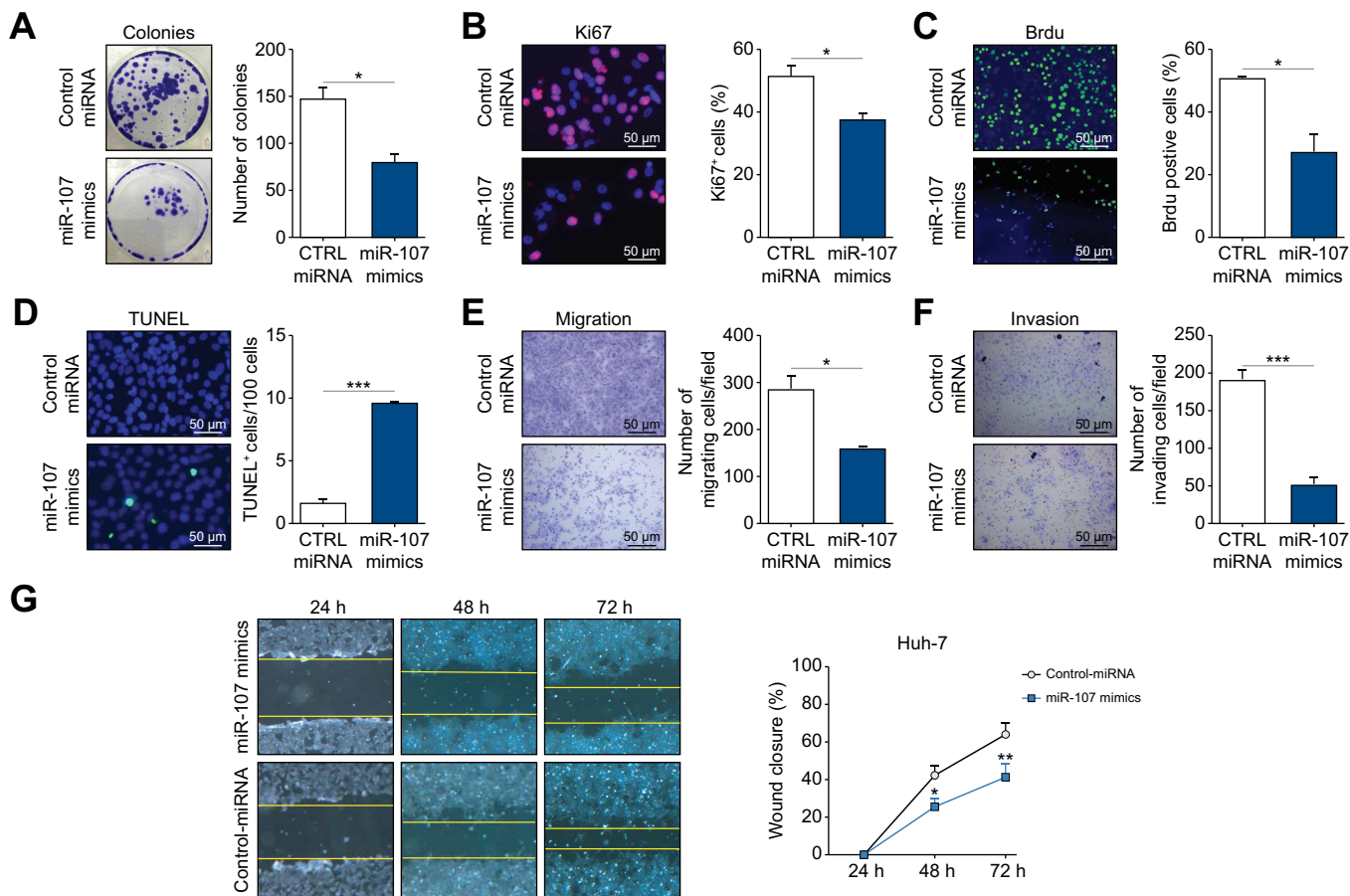


Fig. 2. miR-107 upregulation negatively impacts the fitness of human hepatoma cells. Huh7 cells were transfected with either miR-107 mimic or control miRNA and the effect of miR-107 upregulation on cancer hallmark of hepatoma cells was assessed by (A) colony formation assay (n = 4), (B) Ki-67 staining (n = 5), (C) BrdU proliferation assay (n = 5), (D) while Huh-7 viability was measured by TUNEL assay (n = 5). Transwell migration assay (E) or Transwell coated with Matrigel invasion assay (F) for Hepa1c1c7 cells was determined after transfection with miR-107 mimic or control miRNAs for 72 h (n = 3). (G) Wound-healing assay was performed on Huh7 cells transfected with miR-107 mimic and wound closure was monitored over the indicated time post-transfection after treatment with Mitomycin C for 2 h (n = 3). Representative images are shown for the different experiments. Results are represented as mean ± SD, significant differences were evaluated by using two-tailed, unpaired t test. (*p ≤ 0.05; **p ≤ 0.01; ***p ≤ 0.001).

***In silico* prediction and integration with transcriptome data identified the mitotic spindle associated protein Kif23 as a downstream target of miR-107**

To identify miR-107-responsive genes that may mediate its effects on hepatocarcinogenesis, we analyzed transcriptomic data from the livers of the DEN, AlbLT α/β , and Tet-O-Myc models (GSE102417;¹¹) (see supplementary materials and methods). This led to the identification of 60 genes significantly upregulated in tumor tissue compared to both control and NTL tissues (Fig. 3A, Table S2A). We then cross-referenced these genes with the predicted miR-107 targets from the miRWalk target prediction algorithm,¹⁶ generating a list of 23 putative miR-107 targets (Table S2B). Next, we uploaded this respective gene list into distinct gene set-enrichment tools (*i.e.*, g:Profiler²⁷ and ShinyGo¹⁵) and performed gene set-enrichment analyses (GSEAs). The GSEA results showed that the miR-107 putative target genes had good enrichment scores and reached significance in cell cycle- and mitotic spindle-associated pathways (Fig. 3B and S3A). Additionally, the Disease.Jensen.DISEASES database, which is linked to the ShinyGO platform, revealed that HCC was the primary disease pathway affected by the predicted miR-107 targets (Fig. S3B), further underlining the pathophysiological role of miR-107 in human hepatocarcinogenesis.

To focus on the most promising candidates, the six most significantly enriched genes in the GSEA were selected for further testing: Kif23, Aurkb (aurora kinase B), Prc1 (polycomb repressive complex 1), Ttk (monopolar spindle 1), Anln (anillin), and Nuf2 (nuclear filament-containing protein 2). To assess their relevance in humans, we analyzed the TCGA-LIHC cohort and performed individual Kaplan-Meier analyses to predict overall patient survival for each gene (Fig. S3C). This respective analysis revealed a negative correlation between the expression level of all these respective genes with patient survival, suggesting a prognostic value of KIF23, AURKB, PRC1, TTK, ANLN, and NUF2 in human liver cancer. Additionally, analyses of independent cohorts obtained from the GEO (GSE6764;²⁸; Fig. S3D) showed the significant upregulation for KIF23, AURKB, TTK, ANLN, and NUF2, in the livers of patients with advanced and very advanced HCC, underlining their potential role in human hepatocarcinogenesis.

To further investigate the potential association between these respective genes and human liver cancer, correlations between gene expression and clinical parameters were analyzed using data from TCGA-LIHC cohort (Table S3A). While gene expression was significantly higher in tumors compared to control samples, no significant differences were found between different tumor stages (Fig. S4A). Furthermore, no significant correlation was found between any of these genes and alpha-fetoprotein, bilirubin, serum albumin, or creatinine (Fig. S4B–E), suggesting that these genes are upregulated in tumors but do not correlate with liver function markers or disease severity.

We next used the TargetScan algorithm²⁹ to perform a conservation analysis of miR-107 responsive elements in the 3' untranslated regions (3'-UTRs) of *Kif23*, *Aurkb*, *Ttk*, *Anln*, and *Nuf2*. Remarkably, among the five remaining candidates, only the 3'-UTR of *Kif23* was found to contain a conserved miR-107 responsive elements for miR-107 across multiple species (Fig. 3C). KIF23 is a spindle-associated kinesin crucial for

cytokinesis¹² and is found upregulated in several human malignancies, including colorectal cancer,³⁰ pancreatic,³¹ ovarian cancers,³² and HCC.³³ We therefore measured Kif23 levels in the three mouse models of HCC used in the transcriptomic analysis (*i.e.*, DEN, AlbLT α/β , and Tet-O-Myc HCC models), and confirmed that Kif23 was significantly upregulated in the tumor tissues of all models, but not in the NTL tissue (Fig. S5A,B). We also measured its expression in other well-established murine liver cancer models (namely: Tak1^{LPC-KO}²², Ikk2/Casp8^{LPC-KO}³⁴, Nemo/Ripk3^{LPC-KO}³⁴, Traf2/Casp8^{LPC-KO}³⁵ and Traf2/Ripk1^{LPC-KO}²⁶), and found it to be significantly upregulated in all these respective HCC models (Fig. S5C). Finally, we analyzed KIF23 expression in different human hepatoma cell lines at the mRNA level (*i.e.*, Huh-7, HepG2, and Hep3B) and found it to be significantly upregulated (Fig. S5D), confirming a common upregulation of KIF23 expression in both murine and human liver cancer cells.

KIF23 is a direct target of miR-107 and promotes replicative fitness of liver cancer cells

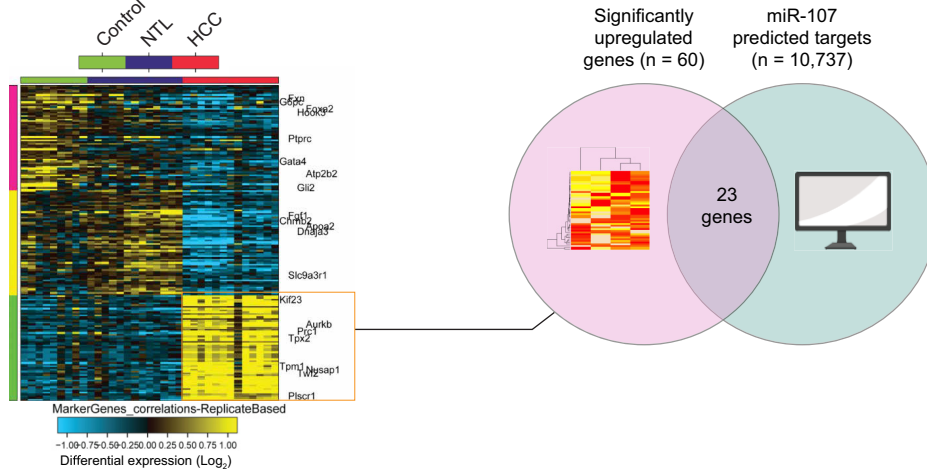
To examine the subcellular localization of KIF23 in hepatoma cells, we performed immunofluorescence analysis with an anti-KIF23 antibody on Huh-7 cells. We found that KIF23 is localized in the nucleus during interphase, relocates to the area of the microtubule-organizing center of the mitotic spindle in dividing cells, and is mainly present in the spindle midzone during anaphase (Fig. 4A), where it is known to be required for the assembly of the myosin contractile ring.¹² To further assess KIF23's role in cytokinesis, we silenced KIF23 expression using RNA interference and observed abnormal cell division characterized by a significant increase in polyploidy in both Huh-7 (Fig. 4B) and HepG2 (Fig. S1D) hepatoma cells.

To further confirm the potential interaction between miR-107 and KIF23, we transfected Huh-7 cells with a GFP vector encoding human miR-107 (Fig. 4C), which resulted in a significant downregulation of KIF23 at both RNA (Fig. 4D) and protein (Fig. 4E) levels. These findings suggested that miR-107 regulates, directly or indirectly, the expression of KIF23. To determine the mechanism through which miR-107 regulates KIF23 expression, the full-length 3'-UTRs of human and mouse KIF23 were cloned downstream of a luciferase reporter gene, either in the original (wild-type) or complementary reverse orientation (as described in³⁶). Upon co-transfection of these constructs with miR-107 mimics into Huh-7 cells, a reduction in luciferase activity was observed specifically in the constructs carrying KIF23-3'UTRs in the native (*i.e.*, WT) orientation. In contrast, no such reduction was seen in the constructs carrying the 3'UTRs in the complementary reverse orientation (Fig. 4F), further supporting the hypothesis that miR-107 directly regulates the expression of KIF23 in both humans and mice.

Next, the functional activity of KIF23 silencing on cellular proliferation and survival was investigated. Consistent with the phenotype observed in response to miR-107 overexpression, small-interfering RNA (siRNA)-mediated inhibition of KIF23 in Huh-7 cells (Fig. 4G) led to a substantial decrease in cellular proliferation, as shown by colony formation (Fig. 4H) and Ki-67 assays (Fig. 4I), and to a significant increase in the number of TUNEL-positive cells (Fig. 4L). Notably KIF23-silencing in HepG2 cells produced comparable results (Fig. S1A–C). In line

miR-107 regulates KIF23 to control tumor cell fitness in HCC

A



B

GO:BP	Term name	Term ID	stats	$-\log_{10}(P_{adj})$	Kif23	Aurkb	Prc1	Ttk	Anln	Nuf2
<input type="checkbox"/>	mitotic cell cycle process	GO:1903047	2.183 × 10 ⁻⁶	6.3	1	1	1	1	1	1
<input type="checkbox"/>	mitotic sister chromatid segregation	GO:0000070	4.323 × 10 ⁻⁶	6.3	1	1	1	1	1	1
<input type="checkbox"/>	sister chromatid segregation	GO:0000819	1.073 × 10 ⁻⁵	5.5	1	1	1	1	1	1
<input type="checkbox"/>	mitotic cell cycle	GO:0000278	1.127 × 10 ⁻⁵	5.5	1	1	1	1	1	1
<input type="checkbox"/>	mitotic spindle midzone assembly	GO:0051256	1.306 × 10 ⁻⁵	5.4	1	1	1	1	1	1
<input type="checkbox"/>	mitotic spindle elongation	GO:0000022	2.284 × 10 ⁻⁵	5.2	1	1	1	1	1	1
<input type="checkbox"/>	cell cycle	GO:007049	3.246 × 10 ⁻⁵	5.1	1	1	1	1	1	1
<input type="checkbox"/>	spindle elongation	GO:0051231	3.653 × 10 ⁻⁵	5.0	1	1	1	1	1	1
<input type="checkbox"/>	nuclear chromosome segregation	GO:0098813	9.702 × 10 ⁻⁵	4.8	1	1	1	1	1	1
<input type="checkbox"/>	mitotic nuclear division	GO:0140014	1.034 × 10 ⁻⁴	4.7	1	1	1	1	1	1
<input type="checkbox"/>	spindle midzone assembly	GO:0051255	1.075 × 10 ⁻⁴	4.7	1	1	1	1	1	1
<input type="checkbox"/>	microtubule cytoskeleton organization involved in mit...	GO:1902850	1.372 × 10 ⁻⁴	4.6	1	1	1	1	1	1
<input type="checkbox"/>	cell cycle process	GO:0022402	1.649 × 10 ⁻⁴	4.5	1	1	1	1	1	1
<input type="checkbox"/>	chromosome segregation	GO:007059	3.179 × 10 ⁻⁴	4.4	1	1	1	1	1	1
<input type="checkbox"/>	cytokinesis	GO:0000910	3.403 × 10 ⁻⁴	4.4	1	1	1	1	1	1
<input type="checkbox"/>	cell division	GO:0051301	4.154 × 10 ⁻⁴	4.3	1	1	1	1	1	1
<input type="checkbox"/>	cytoskeleton-dependent cytokinesis	GO:0061640	1.260 × 10 ⁻³	4.1	1	1	1	1	1	1
<input type="checkbox"/>	nuclear division	GO:0000280	1.397 × 10 ⁻³	4.0	1	1	1	1	1	1
<input type="checkbox"/>	organelle fission	GO:0048285	2.677 × 10 ⁻³	3.8	1	1	1	1	1	1
<input type="checkbox"/>	mitotic spindle organization	GO:007052	3.052 × 10 ⁻³	3.8	1	1	1	1	1	1
<input type="checkbox"/>	positive regulation of cellular process	GO:0048522	5.611 × 10 ⁻³	3.6	1	1	1	1	1	1
<input type="checkbox"/>	chromosome organization	GO:0051276	1.130 × 10 ⁻²	3.4	1	1	1	1	1	1
<input type="checkbox"/>	cytoskeleton organization	GO:007010	1.231 × 10 ⁻²	3.4	1	1	1	1	1	1
<input type="checkbox"/>	regulation of cell cycle	GO:0051726	1.248 × 10 ⁻²	3.4	1	1	1	1	1	1
<input type="checkbox"/>	spindle organization	GO:0007051	1.782 × 10 ⁻²	3.2	1	1	1	1	1	1
<input type="checkbox"/>	positive regulation of biological process	GO:0048518	1.836 × 10 ⁻²	3.2	1	1	1	1	1	1
<input type="checkbox"/>	mitotic cytokinesis	GO:0000281	2.897 × 10 ⁻²	3.0	1	1	1	1	1	1
<input type="checkbox"/>	mitotic spindle assembly	GO:0090307	2.897 × 10 ⁻²	3.0	1	1	1	1	1	1

C

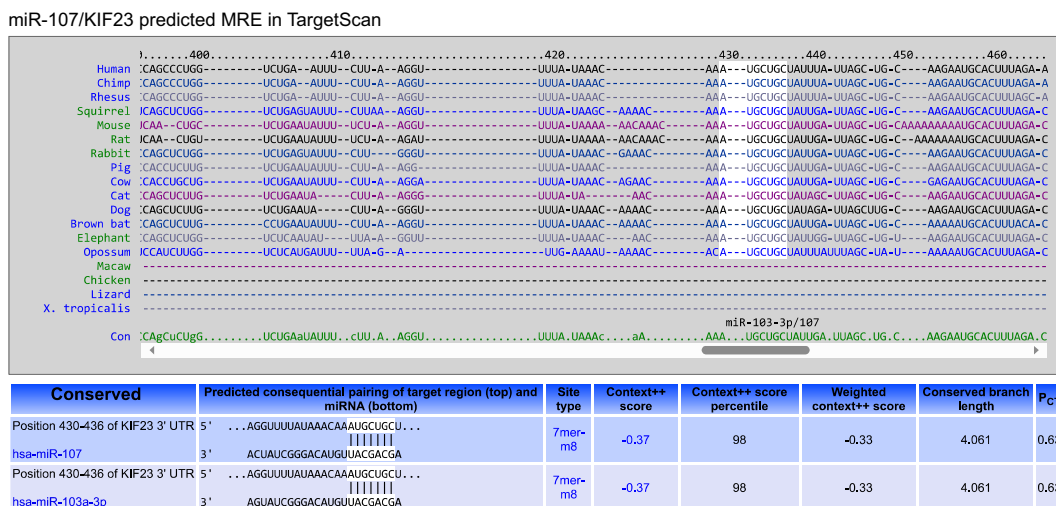


Fig. 3. Kif23, a kinesin involved in cytokinesis, is a conserved direct target of miR-107. (A) Unsupervised hierarchical clustering of the genes regulated in the tumor tissue of the three mouse models used in this study (*i.e.*, DEN, AlbT α / β and Tet-O-Myc) compared to NTL and healthy tissue. The color scale illustrates the fold-change of mRNAs across the samples (Generated by Altanalyze). The overlap between significantly upregulated genes and miRWalk predicted miR-107 targets is shown. (B) G:Profiler enrichment analysis of potential miR-107 targets and the name of the most significantly enriched genes (*i.e.* with the lowest *p* value) is given. (C) TargetScan predicted the presence of a highly conserved binding site for miR-107 in the 3'UTRs of KIF23 across different organisms, including humans, mice and rats. HCC, hepatocellular carcinoma; NTL, non-tumor liver.

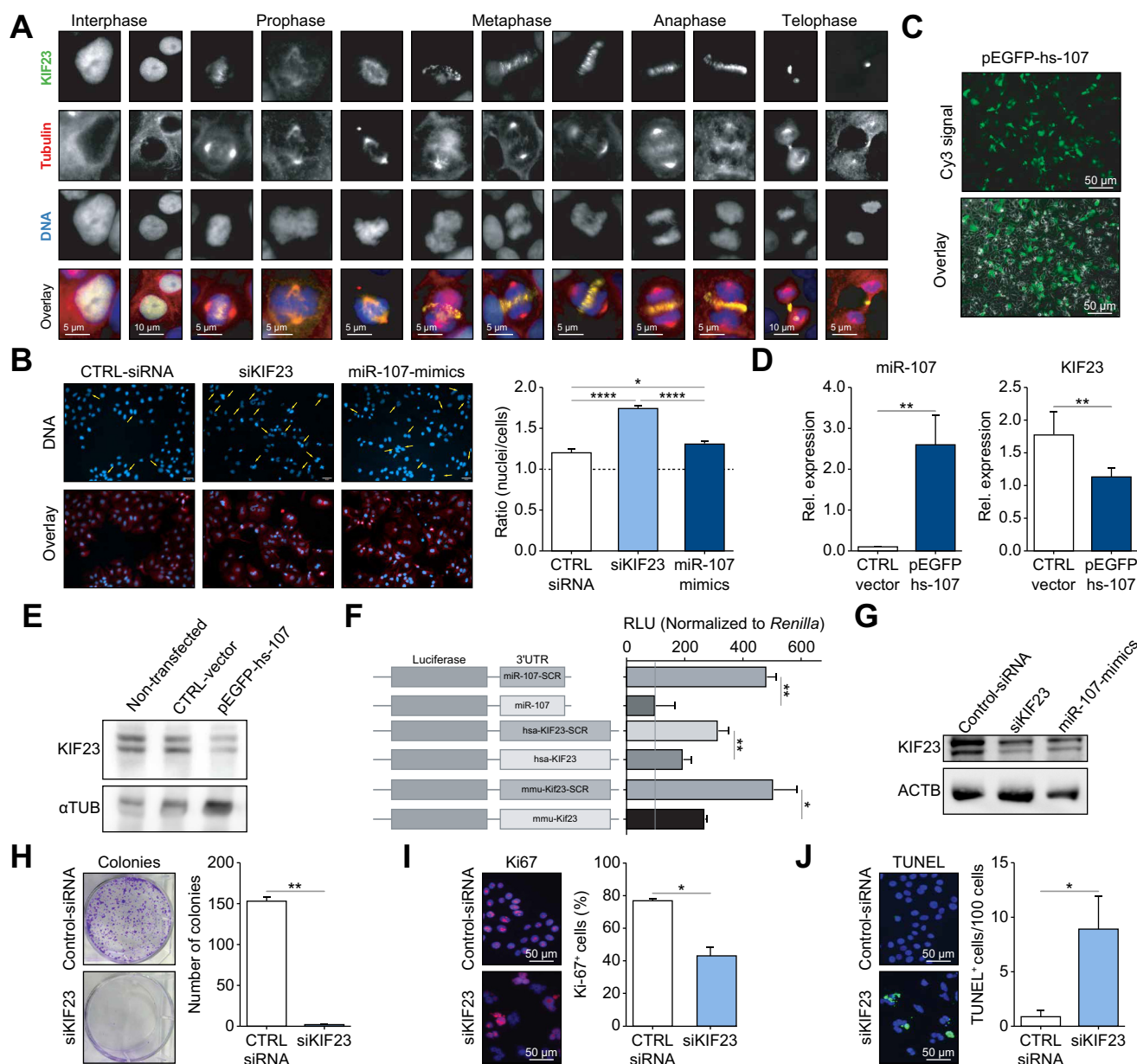


Fig. 4. KIF23 silencing leads to incomplete cytokinesis and impairs survival of cancer cells. (A) Representative images showing KIF23 localization at the different stages of cell cycle (Interphase, Prophase, Metaphase, Anaphase and Telophase) in Huh-7 human hepatoma cells. (B) Both siRNA-mediated silencing of KIF23 and miRNA mimic-induced overexpression of miR-107 were found to impair cytokinesis, leading to cell division defects and an increase in multinucleated cells, as indicated by a significant increase in the cell to nuclei ratio. The number of nuclei and cells were automatically counted using built-in plugins in ImageJ ($n = 5$) (C) In Huh-7 cells transfected with a GFP vector encoding for miR-107 (pEGFP-hs-107) a significant reduction of KIF23 at (D) mRNA and (E) protein levels was observed. (F) The full-length 3'UTRs for the mouse and human KIF23 were cloned into luciferase promoter vector in the sense or in the antisense orientation (SCR). As positive and negative controls, the miR-107 binding site obtained from miRBase was cloned into the 3'UTR of the pMIR vector in either its sense (miR-107, positive control) or antisense (miR-107-SCR, negative control) orientation. Plasmids were transfected into HEK293 cells in the presence or absence of miR-107 mimic and luciferase activity was measured 24 h post-transfection. Relative luciferase activities are shown as percentage of the miR-107 plasmid as transfection control ($n = 4$). (G) Huh-7 cells were transfected with either control-siRNA, anti-KIF23 siRNA (siKIF23) or miR-107-mimics and the effect on KIF23 was evaluated by western blot. Effect of KIF23 silencing on Huh-7 fitness was assessed by (H) colony formation assay ($n = 4$), while Huh-7 proliferation and viability were respectively assessed by (I) Ki-67 staining ($n = 5$) and (J) TUNEL assay ($n = 5$). Results are represented as mean \pm SD, significant differences were evaluated using one-way ANOVA with Newman-Keuls *post hoc* test or using two-tailed, unpaired t test as appropriate. * $p < 0.05$; ** $p < 0.01$; *** $p < 0.001$.

with these results, overexpression of KIF23 was able to rescue proliferative fitness in both Huh-7 (Fig. S6A-C) and HepG2 (Fig. S6D-F) cells transfected with either anti-KIF23 siRNA or miR-107 mimics, indicating that KIF23 is a key functional mediator of miR-107 and that upregulation of KIF23 is required

to support the observed changes in hepatoma cell proliferation and survival. To provide further evidence for a collaborative function of these genes in hepatocarcinogenesis, we analyzed miR-107 and KIF23 expression levels in RNA isolated from human tissues obtained from resected livers in which the tumor

and healthy distal tissues were either from different patients (*i.e.*, unpaired; Fig. 5A, Table S1A) or from the same patient (*i.e.*, paired; Fig. 5B and S7B, Table S1B). This analysis confirmed that miR-107 was significantly downregulated and KIF23 was significantly upregulated in the livers of patients with HCC. Finally, in order to explore the functional relationship between miR-107 and KIF23 in patient survival, a Cox proportional hazards analysis was performed on the sequencing and survival data from TCGA-LIHC cohort. This analysis showed that patients with both higher miR-107 expression and lower KIF23 expression had significantly higher overall survival compared to other combinations. Conversely, the lowest overall survival was observed in patients with low miR-107/high KIF23 expression in their liver (Fig. 5C).

We also tested whether there was an association between the dysregulation of the miR-107/KIF23 axis and the liver disease entity underlying hepatocarcinogenesis using data available in the TCGA-LIHC cohort. For this purpose, miR-107 and KIF23 expression levels were stratified by viral vs. non-viral hepatitis (Fig. S7A, left panel, and Table S3A) or by alcohol-related vs. non-alcohol-related metabolic liver disease (Fig. S7A, right panel, and Table S3A), depending on the available data. Notably, no significant entity-specific regulation pattern of miR-107 or KIF23 was identified in this analysis.

KIF23 nuclear localization is increased in human HCC tissue

Our data suggested that KIF23 is a key functional mediator of miR-107 in both murine and human HCC by supporting cancer cell fitness. To determine whether the increase in mRNA corresponded to an increase in protein levels in human HCC and to assess potential differences in the subcellular localization of KIF23, KIF23 was analyzed in TMA's containing cores from the livers of 62 different patients with HCC.¹⁸ For the assessment of KIF23 levels, TMA's were stained with an anti-KIF23 antibody, and the score was calculated based on KIF23 localization and signal intensity in the tumor tissue (HCC; Fig. 5D; as described in¹⁹) and in the surrounding liver (Fig. 5E and Table S4). This analysis revealed a significant increase in KIF23 expression within the nuclei of the cells localized within the tumor compared to non-tumor tissues (Fig. 5F), providing further evidence that KIF23 plays a role in human hepatocarcinogenesis.

To further explore regulatory relationships between miR-107/KIF23 and genes controlling pathways known to promote cancer growth, Pearson correlation analysis was used to evaluate potential associations between miR-107/KIF23 on one hand and TP53 (tumor protein p53), MYC (MYC proto-oncogene), NRAS

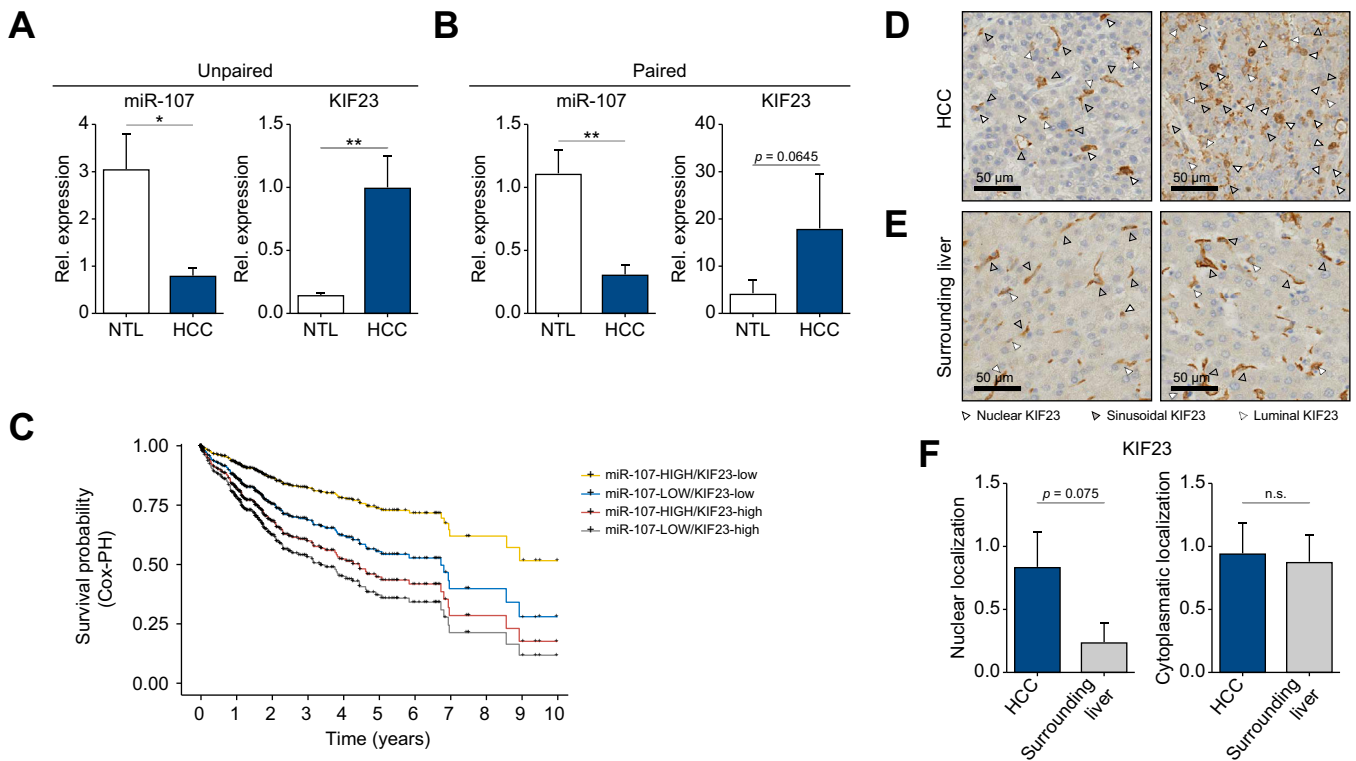


Fig. 5. KIF23 is upregulated in tumor tissues compared to surrounding NTL tissues in patients with HCC. Independent validation of HCC-associated changes in miR-107 and KIF23 expression levels. miR-107 and KIF23 were analyzed by RT-qPCR in both tumor (HCC) and NTL tissues from two different cohorts of (A) unpaired (NTL, n = 7; HCC, n = 7) and (B) paired (n = 9) patients. (C) Cox proportional hazards analysis was performed to evaluate the combined effect of miR-107 and KIF23 expression levels on the overall survival of the cohort of patients with HCC from TCGA repository. The analysis revealed that patients with higher expression of miR-107 and lower expression of KIF23 had the highest probability of survival (p = 0.003). Representative images of TMA's prepared with cores of livers of human patients with HCC from (D) tumor tissue and (E) surrounding liver. KIF23 was detected in both the cytosol and nuclei of liver cells. (F) Higher hepatocyte-specific nuclear KIF23 expression (white arrow) was detected in the HCCs compared to the surrounding normal liver tissues, which instead showed mainly sinusoidal expression of KIF23 (grey arrow). Some HCCs displayed KIF23 luminal staining (dashed arrow), barely observed in surrounding liver. Weak expression of cytoplasmatic KIF23 was seen in both liver tissue types, without significant differences. Results are represented as mean ± SD, significant differences between paired and unpaired samples were evaluated by using two-tailed, unpaired t tests. Survival curves for miR-107 and KIF23 were compared using the Wilcoxon signed-rank test (n.s. = not significant; *p ≤ 0.05; **p ≤ 0.01). HCC, hepatocellular carcinoma; NTL, non-tumor liver.

(neuroblastoma RAS), AKT1 (AKT serine/threonine kinase 1), SMAD4 (mothers against decapentaplegic homolog 4), and TGF- β 1 (transforming growth factor beta 1) on the other. While miR-107 showed no significant correlations, KIF23 levels showed a significant positive correlation with the expression of the respective genes (Fig. S7C, Table S3B).

Targeting the miR-107/KIF23 axis inhibits oncogene-induced liver cancer formation

Given the pronounced impact of miR-107 and its target Kif23 on fundamental biological characteristics of liver cancer cells, we investigated whether manipulating their expression could affect the progression and proliferation of liver cancer in a preclinical HCC model. To induce liver cancer in mice, we employed hydrodynamic tail vein injection (HDTVi) to administer a transposon vector (CaMINmE5') encoding the c-Myc/NRAS oncogenes (which was shown to give rise to highly aggressive HCCs³⁷) in the presence of either a short-hairpin RNA (shRNA) targeting KIF23, a pre-miR-107, or a miR-30e backbone as negative control (miRE). For this, the SplashRNA algorithm³⁸ was used to design three distinct shRNAs targeting various regions of murine Kif23 cDNA, which were then cloned into the RT3GEPIR entry vector.³⁹ Vectors carrying the shRNAs and the pre-miR-107 were transfected into murine Hepa1-6 hepatoma cells, and their efficacy in targeting Kif23 was assessed by western blot (Fig. S8A,B). The most efficient shRNA in targeting Kif23 (shKif23-675), pre-miR-107, and the miRE were cloned into the CaMINmE5' vector as previously described.¹¹ The resulting constructs were co-injected with a

vector expressing the transposase into the tail veins of 7-week-old male C57BL/6j mice using HDTVi. Animals were euthanized 6 weeks after injection, and their livers were examined for tumor presence.

As expected, no tumors were detected in the livers of untreated animals at either the macroscopic or microscopic level (Fig. 6A, S9A and S10A). Conversely, HDTVi of the c-Myc/NRAS oncogene in combination with the control miRNA (camiM-miRE) led to the development of large tumors with morphological features of HCC (Fig. 6B, S9B and S10B). Notably, this corresponded to a significant increase in the liver-to-body weight ratio for this group of animals, which is a quantitative surrogate for both tumor mass and tumor development (Fig. S11A, Table S5A). Furthermore, the effect of the different HDTVi-injected transposonal vectors on liver cancer development was confirmed both by the measurements of AST (aspartate aminotransferase) and ALT (alanine aminotransferase) and by the quantification of c-Myc, NRAS, KIF23 and miR-107 (Fig. S11B,C, Table S5B).

Notably, while the macroscopic examination of the livers of animals administered with the vector encoding for c-Myc/NRAS in combination with miR-107 (camiN-pre107) did not reveal any apparent tumors (Fig. 6C upper panel and S9C), histological analysis of these livers uncovered well-defined masses of basophilic cells, indicative of early tumor development (Fig. 6C lower panel and S10C). Finally, mice injected with vectors carrying the oncogene in combination with anti-Kif23 shRNA (shKif23-675) were completely tumor-free both macroscopically and microscopically (Fig. 6D, S9D, and S10D, Table S6).

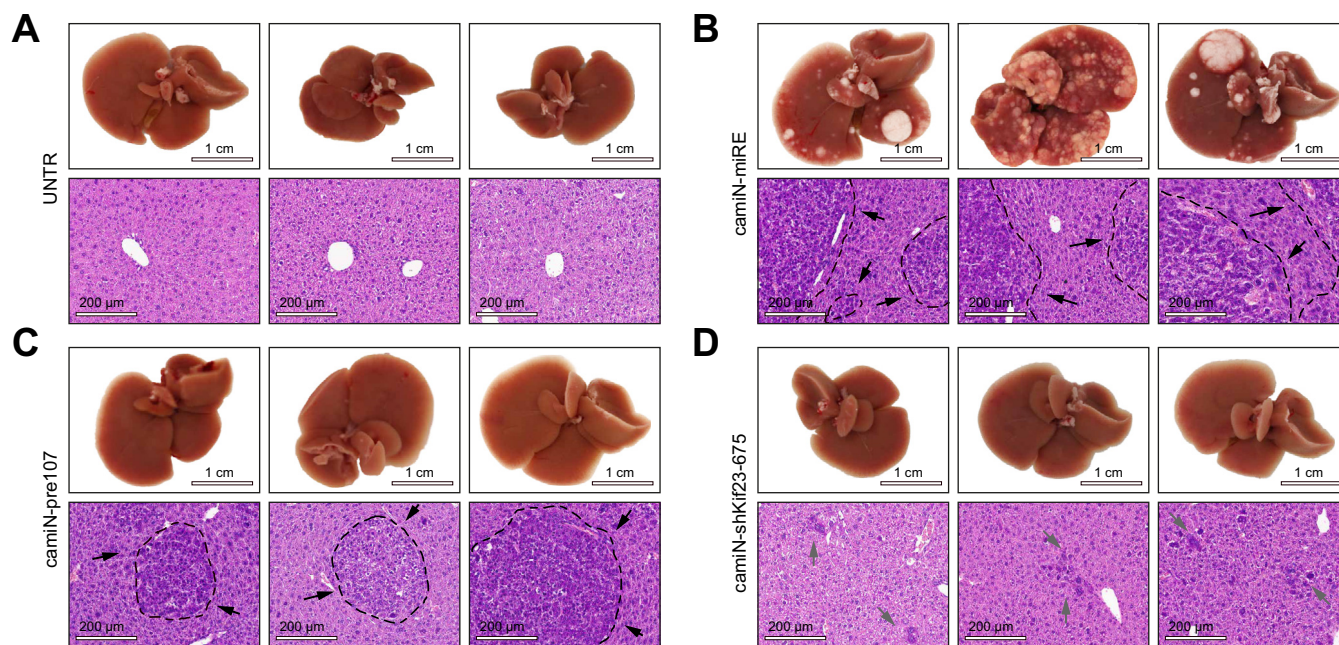


Fig. 6. Targeting the miR-107/Kif23 axis prevents the formation of oncogene-induced liver cancer. Representative macroscopic images (top panels) and microscopic images (lower panels) of the tumor burden in the livers of control untreated mice (UNTR; A) and in the livers of mice 6 weeks after HDTVi-mediated administration of transposonal vectors carrying the c-Myc/NRAS oncogenes, in conjunction with either the control miRNA (camiN-miRE; B), the pre-miR-107 (camiN-pre107; C), or the anti-Kif23 shRNA (camiN-shKif23-675; D), are presented. Tumors were exclusively visible in the macroscopic pictures of the livers from camiN-miRE animals. However, microscopic images revealed the presence of liver cancer in animals injected with both the camiN-miRE and camiN-pre107 vectors (black arrows). In contrast, the livers of camiN-shKif23-675-injected animals remained tumor-free in both macroscopic and microscopic images. Notably, a small number of atypical cells were detected in the livers of camiN-shKif23-675-injected animals (grey arrows). Microscopic images were captured at 20x magnification. UNTR, untreated animals.

Finally, to assess the impact of miR-107 overexpression and KIF23 silencing on the immune cell landscape of the liver, tissue sections were stained with antibodies against F4/80 (macrophages), B220 (B cells) and CD3 (T cells). Of these, macrophages were found to be significantly reduced in the livers of animals injected with either camiN-miRE or camiN-pre107, but not in the livers of animals injected with camiN-shKif23-675 (Fig. 7A,B). B220 staining revealed a significant increase in infiltrating B cells exclusively in the livers of mice injected with the camiN-miRE vector (Fig. 7C,D), while the spatial distribution and number of T cells remained essentially unchanged (Fig. S12). While the functional role of immune cells in the mediation of the phenotype is not fully clear at present, these results indicate that the functions of macrophages/monocytes in the liver could be altered by a possible uptake of

the vectors. However, based on the functional data in hepatoma cells and the high expression in hepatocytes vs. other cell types in the liver, it is likely that the phenotype observed in our models was mediated through direct effects on tumor cells rather than on immune cells.

Discussion

There has been significant progress in the systemic treatment of HCC in recent years.⁴⁰ However, this was mainly the result of newly established concepts in other tumors, namely immunotherapy, being transferred successfully to HCC in clinical trials.^{2,3} Meanwhile, a large amount of data has been collected in experimental mouse models and has revealed new, promising targets that have not yet been successfully tested in early

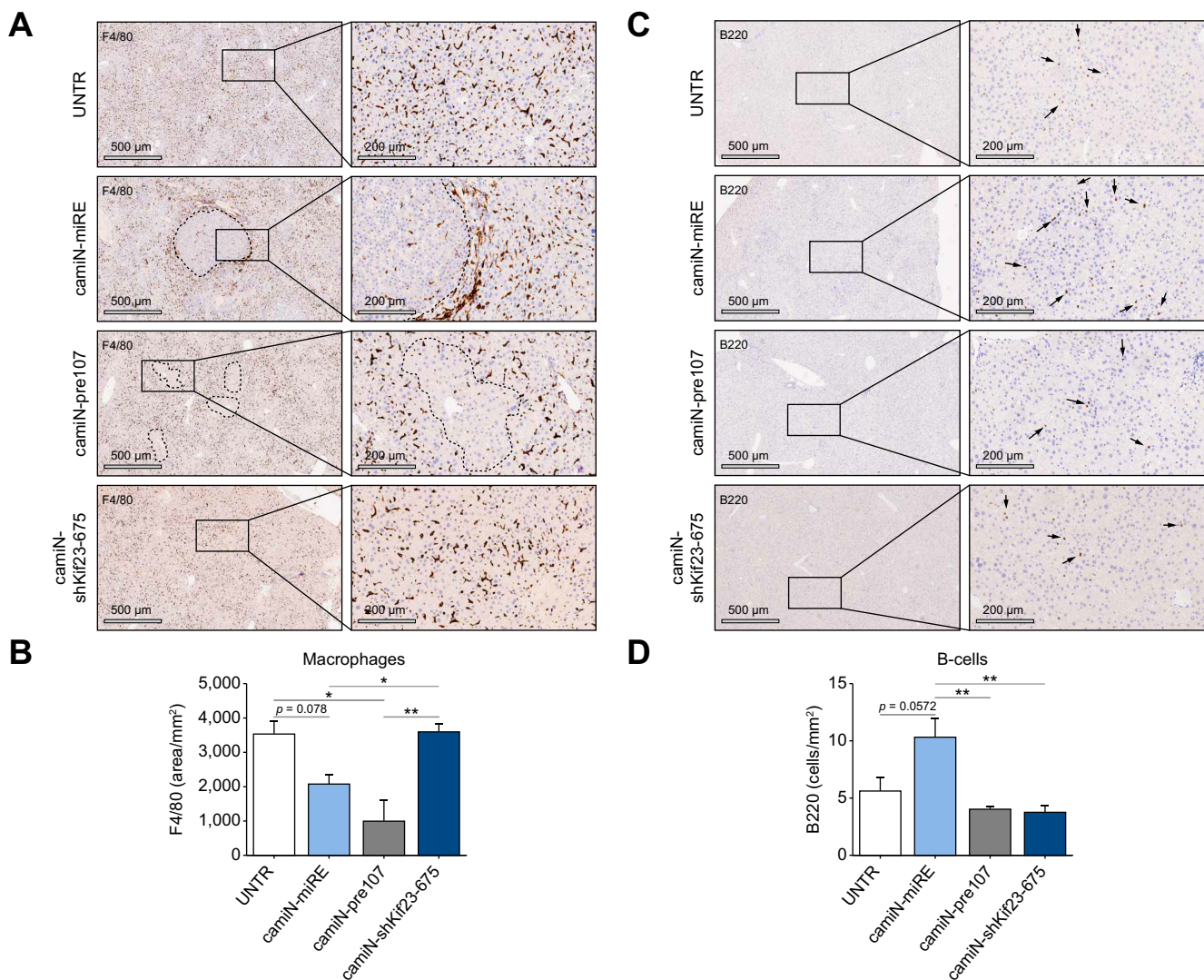


Fig. 7. F4/80 and B220 staining of liver tissue from HDTV and control mice. (A) F4/80 staining did not show altered inflammation in the livers of UNTR and mice injected with the transposonal vectors carrying the c-Myc/NRAS oncogenes anti-Kif23 shRNA (camIN-shKif23). A significant reduction in the number of macrophages was detected in the livers of mice 6 weeks after the HDTV-mediated administration of transposonal vectors carrying the c-Myc/NRAS oncogenes in combination with either the control miRNA (camIN-miRE) or the pre-miR-107 (camIN-pre-107). The left panel shows representative images at different magnification. (B) Quantification of F4/80 signals. (C) B220 staining altered inflammation/distribution pattern in the livers of any of the animals included in the study. (D) Quantification of B220 positive cells. Results are represented as mean ± SD, significant differences were evaluated by using 1-way ANOVA with Newman-Keuls *post hoc* test (**p* ≤ 0.05; ***p* ≤ 0.01). camIN-miRE, animals injected the vectors encoding for the c-Myc/NRAS oncogenes and control miRNA; camIN-pre-107, animals injected with the vectors encoding for pre-miR-107; camIN-shKif23-675, animals injected with the oncogenes and anti-Kif23 shRNA; UNTR, untreated animals.

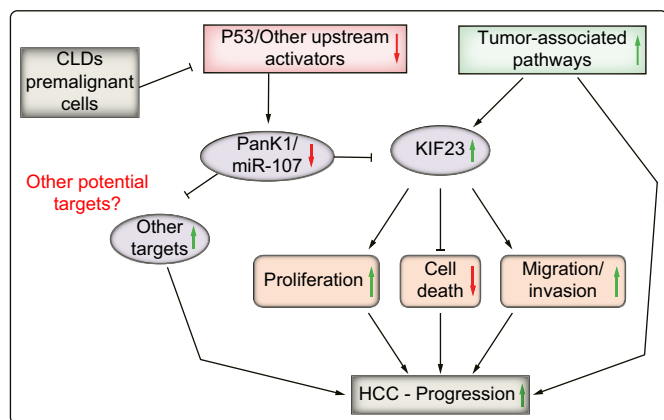


Fig. 8. Proposed model for the role of miR-107/KIF23 axis deregulation in liver cancer. Proposed model for the regulation of the miR-107/KIF23 axis in liver cancer. We propose that miR-107 levels are downregulated in CLDs and in pre-malignant and malignant cells due to deregulation of P53, a known upstream regulator of Pank1/miR-107 transcription, or activation/inhibition of yet to be identified signaling pathways that modulate miR-107 biogenesis. This down-regulation leads to the upregulation of miR-107 targets, including KIF23, whose expression is activated by tumor-associated pathways. Although KIF23 is not classified as an oncogene, it supports cell division by promoting cytokinesis. This enhances the fitness of cancer cells, leading to a significant increase in proliferation and migration, and indirectly reducing cell death. Thus, the dysregulation of the miR-107/KIF23 axis plays a critical role in promoting tumor cell fitness, thereby exacerbating HCC progression and pathogenesis. CLDs, chronic liver diseases; HCC, hepatocellular carcinoma.

clinical trials. One possible reason for this massive translational gap could be the limitations inherent in the transfer of data from individual mouse models with their specific limitations.^{41,42} In our current approach, we could systematically increase the probability of successful translation by integrating several pathogenically different mouse models and thus identifying a signaling pathway that is highly relevant as a biomarker and potential target in human HCC.

Our data identified miR-107 as a master regulator of liver cancer cell fitness by controlling cytokinesis of tumor cells through Kif23 (Figs 4F and 6). Of note, miR-107 expression has been implicated in various human cancers, but data were conflicting regarding a tumor-suppressing vs. tumor-promoting effect.^{43–45} Also in liver cancer, previous studies reported both carcinogenic⁴⁶ and tumor-suppressive effects of miR-107.^{47,48} We found that lower miR-107 expression correlated with enhanced fitness of human and mouse hepatoma cells and significantly lower survival in patients with HCC.

We sought to identify miR-107-regulated genes that act as functional mediators of its activity in supporting the fitness of cancer cells. Through comprehensive approaches combining system biology and experimental validation, we identified KIF23, a spindle-associated microtubule motor protein, as a novel direct target of miR-107. KIF23 is a key component of the centralspindlin complex, which is required for central spindle assembly and cytokinesis.⁴⁹ KIF23 plays a crucial role in cell division, particularly during mitosis, where it is required for the formation of the contractile ring and the subsequent cleavage of the cell membrane of the two daughter cells. Regarding its potential role in cancer, elevated KIF23 levels have been observed in a number of human cancers, including HCC,³³ colorectal cancer,³⁰ pancreatic ductal adenocarcinoma,³¹ and ovarian cancers,³² where high levels of KIF23 have been

associated with poor prognosis. Although the precise mechanisms through which KIF23 influences cancer development and progression are not fully understood, it has been suggested that KIF23 *per se* does not promote tumorigenesis or oncogenic transformation. Therefore, we propose that KIF23 enhances tumor cell fitness by supporting cellular division, which indirectly promotes tumor cell proliferation. Through our work, we showed that high expression levels of KIF23 were associated with the malignant behavior of human hepatoma cells and correlated with unfavorable clinical outcomes in cohorts of patients with LIHC. Notably, through the analysis of TMA prepared from the liver cores of patients with HCC, we could show that KIF23 protein accumulates in the nuclei of tumor cells compared to the nuclei of cells localized in the surrounding, non-tumorigenic tissue, which might represent an important feature when validating its potential role as a tissue-biomarker in human HCC.

Recently, methods to inactivate spindle-associated kinesins have been investigated because silencing specific members of this class of motor proteins could provide an effective therapy against cancer.⁵⁰ However, despite promising *in vitro* data, early clinical trials targeting the centromere protein E, or the kinesin spindle protein (KSP/also known as Eg5) did not reflect the positive preclinical findings.^{51–53} These setbacks highlight the need to explore alternative approaches and methods for targeting this category of proteins. In this respect, our discovery that shRNA-mediated silencing of Kif23 prevented c-Myc/NRAS-induced liver cancer formation *in vivo* suggests that Kif23 might be a promising new target.

It is interesting to note that – despite the complete absence of macroscopic and microscopic tumors – some small abnormalities were detected in the histological analysis of livers from those mice injected with anti-Kif23 shRNAs (Fig. 6D lower panel and S10D). These abnormalities might represent dysplastic foci containing a small number of atypical cells, indicating that the oncogene-induced neoplastic process in the cells receiving the transposon vectors was halted early, hence preventing the formation of fully fledged lesions. These dysplastic foci might be linked to the immune-mediated clearance of pre-malignant senescent parenchymal cells.⁵⁴ Of note, silencing of Kif23 resulted in a “black-and-white” phenotype *in vivo*, while overexpression of miR-107 did not lead to a full rescue from tumor formation. miRNAs are known to modulate, not fully inhibit their target genes. Notably, the findings that KIF23 overexpression rescued the proliferative fitness of both Huh-7 and HepG2 cells *in vitro* (Fig. S6) support the conclusion that KIF23 is one of the main mediators of miR-107 activity in hepatoma cells. Hence, it is possible that the overexpression of miR-107 is not sufficient to suppress Kif23 to the level required to inhibit c-Myc/NRAS-mediated tumor growth, resulting in a delay but not a complete inhibition of tumor formation *in vivo*. Importantly, we cannot completely exclude that other molecules may also mediate the function of miR-107 in hepatocarcinogenesis. To fully elucidate this, combined HDTV_i experiments would be required to show whether Kif23 overexpression can completely reverse the effect of miR-107 overexpression *in vivo*.

Prior research indicated potential risks associated with the modulation of miR-107 *in vivo*. As such, the safety and tolerability of RG-125 (AZD4076), an RNA-based therapeutic specifically targeting miR-107 *in vivo*, was tested in phase I/IIa trial

settings in patients with type 2 diabetes and metabolic dysfunction-associated steatohepatitis (MASH, a term recently adopted to replace non-alcoholic steatohepatitis [or NASH]⁵⁵), based on preclinical findings suggesting a regulatory function on insulin sensitivity.⁵⁶ However, this study was terminated (NCT02826525,⁵⁷), and an independent study demonstrated that targeting miR-103/-107 might adversely affect cardiac function and metabolism.⁵⁸ This observation together with our data suggests that silencing KIF23 rather than modulating miR-107 might be a more specific approach with less side

effects *in vivo*. It should be noted that the HDTV_i method used in this study is not suitable for delivering RNA therapeutics to humans. Therefore, alternative delivery strategies, such as lipid nanoparticles,⁵⁹ engineered extracellular vesicles,⁶⁰ or conjugated siRNA,⁶¹ should be investigated for their efficacy in delivering RNA therapeutics targeting KIF23 *in vivo*.

In summary, our study, as illustrated in Fig. 8, unveils the crucial role played by the dysregulation of the miR-107/KIF23 axis in promoting tumor cell fitness and, thereby exacerbating HCC pathogenesis.

Affiliations

¹Department of Gastroenterology, Hepatology and Infectious Diseases, Medical Faculty, Heinrich Heine University Düsseldorf, Germany; ²Center for Integrated Oncology Aachen Bonn Cologne Düsseldorf (CIO ABCD), Düsseldorf, Germany; ³Institute of Pathology, University Hospital of Heidelberg, Heidelberg, Germany; ⁴Department of Surgery and Transplantation, University Hospital RWTH Aachen, Aachen, Germany; ⁵Department of Surgery and Transplantation, University Hospital Essen, Essen, Germany; ⁶Department of Pathology, Erasmus Medical Center Rotterdam, The Netherlands; ⁷Leibniz Research Centre for Working Environment and Human Factors, Technical University Dortmund, Ardeystr. 67, Dortmund, Germany; ⁸Forensic Medicine and Toxicology Department, Faculty of Veterinary Medicine, South Valley University, Qena, Egypt; ⁹Department of Surgery, Heinrich-Heine-University and University Hospital Düsseldorf, Germany; ¹⁰Department of Internal Medicine VIII, University Hospital Tübingen, Tübingen, Germany; ¹¹Division of Chronic Inflammation and Cancer, German Cancer Research Center (DKFZ), Heidelberg, Germany

Abbreviations

3'-UTRs, 3' untranslated regions; DEN, diethylnitrosamine; GEO, Gene Expression Omnibus; GSEA, gene set-enrichment analysis; HCC, hepatocellular carcinoma; HDTV_i, hydrodynamic tail vein injection; KIF23, kinesin family member 23; LIHC, liver hepatocellular carcinoma; miRE, miR-30e backbone as negative control; miRNA, microRNA; NTL, non-tumor liver; shRNA, short-hairpin RNA; siRNA, small-interfering RNA; TCGA, The Cancer Genome Atlas; TMA, tissue microarray; WT, wild-type.

Financial support

This work was supported by a grant of the German Research Foundation (Deutsche Forschungsgemeinschaft) to M.C. and T.Lu (Reference: CA 830/3-1). T.Lu. was further funded by the European Research Council (ERC) under the European Union's Horizon 2020 research and innovation program through the ERC Consolidator Grant 'PhaseControl' (Grant Agreement 771083). T.Lu. was also funded by the German-Research-Foundation (DFG – LU 1360/3-2 (279874820), LU 1360/4-(1461704932) and the German Ministry of Health (BMG – DEEP LIVER 2520DAT111). M.V. and T.Lu were funded by the German Cancer Aid (Deutsche Krebshilfe 70114893) and received funding from the Ministry of Culture and Science of the State of North Rhine-Westphalia (CANTAR – NW21-062E). C.R. received funding from the Sander Stiftung (2017.134.1).

Conflicts of interest

The authors have no relevant financial or non-financial interests to disclose. Please refer to the accompanying ICMJE disclosure forms for further details.

Authors' contributions

M.C., C.R. and T.Lu., designed and guided the research. M.C. and T.Lu., wrote the manuscript with help from other authors. M.C., performed and analyzed most of the experiments. S.R., C.A., R.P., M.V., M.T.S., V.D., M.A.D, S.D.W., J.G.B., and C.R., contributed to research design and/or conducted experiments. A.G., W.A., and J.G.H. provided PHH cells. L.R.H, U.P.N, G.F. and W.T.K., provided liver resections from HCC patients. L.Z. and M.H., provided important technical support. R.P., L.R.H, U.P.N., and T.Lo., generated and analyzed the Tissue microarrays. T.Lo., conducted histo-pathological analyses. All the authors read and approved the manuscript.

Data availability statement

All data used in this study have been included in the manuscript.

Acknowledgements

The authors are grateful to Claudia Rupprecht, Nicole Eichhorst, Stefanie Lindner, Michaela Fastrich, Torsten Janssen and Nathalie Walter for the technical assistance, and to Jenny Hetzer (HistoCore, Medical University Tübingen) for the immune staining of the mouse livers. The authors thank the Center of Model System

and Comparative Pathology (CMCP) at the Institute of Pathology in Heidelberg for their technical assistance in human tissue staining and the Tissue Bank of the National Center of Tumor Diseases (NCT, Heidelberg) for the tissue slide scanning.

Supplementary data

Supplementary data to this article can be found online at <https://doi.org/10.1016/j.jhep.2024.08.025>.

References

Author names in bold designate shared co-first authorship

- [1] Llovet JM, Kelley RK, Villanueva A, et al. Hepatocellular carcinoma. *Nat Rev Dis Primers* 2021;7:6.
- [2] Llovet JM, Castet F, Heikenwalder M, et al. Immunotherapies for hepatocellular carcinoma. *Nat Rev Clin Oncol* 2022;19:151–172.
- [3] Mandlik DS, Mandlik SK, Choudhary HB. Immunotherapy for hepatocellular carcinoma: current status and future perspectives. *World J Gastroenterol* 2023;29:1054–1075.
- [4] McGlynn KA, Petrick JL, El-Serag HB. Epidemiology of hepatocellular carcinoma. *Hepatology* 2021;73(Suppl 1):4–13.
- [5] Boshuizen J, Peeper DS. Rational cancer treatment combinations: an urgent clinical need. *Mol Cell* 2020;78:1002–1018.
- [6] Tan AC, Bagley SJ, Wen PY, et al. Systematic review of combinations of targeted or immunotherapy in advanced solid tumors. *J Immunother Cancer* 2021;9.
- [7] Dhawan A, Scott JG, Harris AL, et al. Pan-cancer characterisation of microRNA across cancer hallmarks reveals microRNA-mediated down-regulation of tumour suppressors. *Nat Commun* 2018;9:5228.
- [8] Callegari E, Gramantieri L, Domenicali M, et al. MicroRNAs in liver cancer: a model for investigating pathogenesis and novel therapeutic approaches. *Cell Death Differ* 2015;22:46–57.
- [9] Chan LK, Tsui YM, Ho DW, et al. Cellular heterogeneity and plasticity in liver cancer. *Semin Cancer Biol* 2022;82:134–149.
- [10] Anastasiadou E, Jacob LS, Slack FJ. Non-coding RNA networks in cancer. *Nat Rev Cancer* 2018;18:5–18.
- [11] Roy S, Hooiveld GJ, Seehawer M, et al. microRNA 193a-5p regulates levels of nucleolar- and spindle-associated protein 1 to suppress hepatocarcinogenesis. *Gastroenterology* 2018;155:1951–1966 e1926.
- [12] Nislow C, Lombillo VA, Kuriyama R, et al. A plus-end-directed motor enzyme that moves antiparallel microtubules *in vitro* localizes to the interzone of mitotic spindles. *Nature* 1992;359:543–547.
- [13] Patra BG, Roberts K, Wu H. A content-based dataset recommendation system for researchers—a case study on Gene Expression Omnibus (GEO) repository. *Database (Oxford)* 2020;2020:1.
- [14] Emig D, Salomonis N, Baumbach J, et al. AltAnalyze and DomainGraph: analyzing and visualizing exon expression data. *Nucleic Acids Res* 2010;38:W755–W762.

- [15] Ge SX, Jung D, Yao R. ShinyGO: a graphical gene-set enrichment tool for animals and plants. *Bioinformatics* 2020;36:2628–2629.
- [16] Sticht C, De La Torre C, Parveen A, et al. miRWalk: an online resource for prediction of microRNA binding sites. *PLoS One* 2018;13:e0206239.
- [17] Paluschinski M, Schira-Heinen J, Pellegrino R, et al. Uncovering novel roles of miR-122 in the pathophysiology of the liver: potential interaction with NRF1 and E2F4 signaling. *Cancers (Basel)* 2023;15.
- [18] Longerich T, Brehahn K, Odenthal M, et al. Factors of transforming growth factor beta signalling are co-regulated in human hepatocellular carcinoma. *Virchows Arch* 2004;445:589–596.
- [19] Schlaeger C, Longerich T, Schiller C, et al. Etiology-dependent molecular mechanisms in human hepatocarcinogenesis. *Hepatology* 2008;47:511–520.
- [20] Györfy B. Discovery and ranking of the most robust prognostic biomarkers in serous ovarian cancer. *Geroscience* 2023;45:1889–1898.
- [21] Cheng X, Liu Y, Wang J, et al. cSurvival: a web resource for biomarker interactions in cancer outcomes and in cell lines. *Brief Bioinform* 2022;23.
- [22] **Bettermann K, Vucur M**, Haybaeck J, et al. TAK1 suppresses a NEMO-dependent but NF-kappaB-independent pathway to liver cancer. *Cancer Cell* 2010;17:481–496.
- [23] **Vucur M, Reisinger F**, Gautheron J, et al. RIP3 inhibits inflammatory hepatocarcinogenesis but promotes cholestasis by controlling caspase-8- and JNK-dependent compensatory cell proliferation. *Cell Rep* 2013;4:776–790.
- [24] Xin B, Yamamoto M, Fujii K, et al. Critical role of Myc activation in mouse hepatocarcinogenesis induced by the activation of AKT and RAS pathways. *Oncogene* 2017;36:5087–5097.
- [25] Pikarsky E, Porat RM, Stein I, et al. NF-kappaB functions as a tumour promoter in inflammation-associated cancer. *Nature* 2004;431:461–466.
- [26] **Schneider AT, Gautheron J**, Feoktistova M, et al. RIPK1 suppresses a TRAF2-dependent pathway to liver cancer. *Cancer Cell* 2017;31:94–109.
- [27] **Kolberg L, Raudvere U, Kuzmin I**, et al. g:Profiler-interoperable web service for functional enrichment analysis and gene identifier mapping (2023 update). *Nucleic Acids Res* 2023;51:W207–W212.
- [28] Wurmbach E, Chen YB, Khitrov G, et al. Genome-wide molecular profiles of HCV-induced dysplasia and hepatocellular carcinoma. *Hepatology* 2007;45:938–947.
- [29] Agarwal V, Bell GW, Nam JW, et al. Predicting effective microRNA target sites in mammalian mRNAs. *Elife* 2015;4.
- [30] Ji Z, Mi A, Li M, et al. Aberrant KIF23 expression is associated with adverse clinical outcome and promotes cellular malignant behavior through the Wnt/beta-catenin signaling pathway in Colorectal Cancer. *J Cancer* 2021;12:2030–2040.
- [31] **Gao CT, Ren J, Yu J**, et al. KIF23 enhances cell proliferation in pancreatic ductal adenocarcinoma and is a potent therapeutic target. *Ann Transl Med* 2020;8:1394.
- [32] **Hu Y, Zheng M**, Wang C, et al. Identification of KIF23 as a prognostic signature for ovarian cancer based on large-scale sampling and clinical validation. *Am J Transl Res* 2020;12:4955–4976.
- [33] **Saito Y, Yin D**, Kubota N, et al. A therapeutically targetable TAZ-TEAD2 pathway drives the growth of hepatocellular carcinoma via ANLN and KIF23. *Gastroenterology* 2023;164:1279–1292.
- [34] Paluschinski M, Kordes C, Vucur M, et al. Differential modulation of miR-122 transcription by TGFbeta1/BMP6: implications for nonresolving inflammation and hepatocarcinogenesis. *Cells* 2023;12.
- [35] Vucur M, Ghallab A, Schneider AT, et al. Sublethal necroptosis signaling promotes inflammation and liver cancer. *Immunity* 2023;56:1578–1595 e1578.
- [36] Castoldi M, Vujic Spasic M, Altamura S, et al. The liver-specific microRNA miR-122 controls systemic iron homeostasis in mice. *J Clin Invest* 2011;121:1386–1396.
- [37] **Seehawer M, Heinzmann F**, D'Artista L, et al. Necroptosis microenvironment directs lineage commitment in liver cancer. *Nature* 2018;562:69–75.
- [38] Pelossof R, Fairchild L, Huang CH, et al. Prediction of potent shRNAs with a sequential classification algorithm. *Nat Biotechnol* 2017;35:350–353.
- [39] Fellmann C, Hoffmann T, Sridhar V, et al. An optimized microRNA backbone for effective single-copy RNAi. *Cell Rep* 2013;5:1704–1713.
- [40] Chen Z, Xie H, Hu M, et al. Recent progress in treatment of hepatocellular carcinoma. *Am J Cancer Res* 2020;10:2993–3036.
- [41] Wang XW, Thorgerirsson SS. The biological and clinical challenge of liver cancer heterogeneity. *Hepat Oncol* 2014;1:349–353.
- [42] Mak IW, Evaniew N, Ghert M. Lost in translation: animal models and clinical trials in cancer treatment. *Am J Transl Res* 2014;6:114–118.
- [43] Luo Z, Zheng Y, Zhang W. Pleiotropic functions of miR107 in cancer networks. *Onco Targets Ther* 2018;11:4113–4124.
- [44] **Zou CD, Zhao WM**, Wang XN, et al. MicroRNA-107: a novel promoter of tumor progression that targets the CPEB3/EGFR axis in human hepatocellular carcinoma. *Oncotarget* 2016;7:266–278.
- [45] Khan S, Zhang DY, Zhang JY, et al. The key role of microRNAs in initiation and progression of hepatocellular carcinoma. *Front Oncol* 2022;12:950374.
- [46] **Zhang JJ, Wang CY**, Hua L, et al. miR-107 promotes hepatocellular carcinoma cell proliferation by targeting Axin2. *Int J Clin Exp Pathol* 2015;8:5168–5174.
- [47] Wang Y, Chen F, Zhao M, et al. MiR-107 suppresses proliferation of hepatoma cells through targeting HMGA2 mRNA 3'UTR. *Biochem Biophys Res Commun* 2016;480:455–460.
- [48] Chen HA, Li CC, Lin YJ, et al. Hsa-miR-107 regulates chemosensitivity and inhibits tumor growth in hepatocellular carcinoma cells. *Aging (Albany NY)* 2021;13:12046–12057.
- [49] Mishima M, Kaitna S, Glotzer M. Central spindle assembly and cytokinesis require a kinesin-like protein/RhoGAP complex with microtubule bundling activity. *Dev Cell* 2002;2:41–54.
- [50] Henderson MC, Shaw YJ, Wang H, et al. UA62784, a novel inhibitor of centromere protein E kinesin-like protein. *Mol Cancer Ther* 2009;8:36–44.
- [51] Knox JJ, Gill S, Synold TW, et al. A phase II and pharmacokinetic study of SB-715992, in patients with metastatic hepatocellular carcinoma: a study of the National Cancer Institute of Canada Clinical Trials Group (NCIC CTG IND. 168). *Invest New Drugs* 2008;26:265–272.
- [52] Wood KW, Lad L, Luo L, et al. Antitumor activity of an allosteric inhibitor of centromere-associated protein-E. *Proc Natl Acad Sci U S A* 2010;107:5839–5844.
- [53] Chandrasekaran G, Tatrai P, Gergely F. Hitting the brakes: targeting microtubule motors in cancer. *Br J Cancer* 2015;113:693–698.
- [54] Kang TW, Yevsa T, Woller N, et al. Senescence surveillance of pre-malignant hepatocytes limits liver cancer development. *Nature* 2011;479:547–551.
- [55] Rinella ME, Lazarus JV, Ratzin V, et al. A multisociety Delphi consensus statement on new fatty liver disease nomenclature. *J Hepatol* 2023;76:1542–1556.
- [56] Trajkovski M, Hausser J, Soutschek J, et al. MicroRNAs 103 and 107 regulate insulin sensitivity. *Nature* 2011;474:649–653.
- [57] Drenth JPH, Schattenberg JM. The nonalcoholic steatohepatitis (NASH) drug development graveyard: established hurdles and planning for future success. *Expert Opin Investig Drugs* 2020;29:1365–1375.
- [58] Rech M, Kuhn AR, Lumens J, et al. AntagomiR-103 and -107 treatment affects cardiac function and metabolism. *Mol Ther Nucleic Acids* 2019;14:424–437.
- [59] Bottger R, Pauli G, Chao PH, et al. Lipid-based nanoparticle technologies for liver targeting. *Adv Drug Deliv Rev* 2020;154–155:79–101.
- [60] Johnson V, Vasu S, Kumar US, et al. Surface-engineered extracellular vesicles in cancer immunotherapy. *Cancers (Basel)* 2023;15.
- [61] Neumayer C, Ng D, Requena D, et al. GalNAc-conjugated siRNA targeting the DNAJB1-PRKACA fusion junction in Fibrolamellar Hepatocellular Carcinoma. *Mol Ther* 2023;32:140–151.

Keywords: Liver cancer; miR-107; Kif23; tissue microarrays; HDTV1.

Received 9 December 2023; received in revised form 7 August 2024; accepted 22 August 2024; available online 1 September 2024